Optical properties of Ar ions irradiated nanocrystalline ZrC and ZrN thin films

C. Martin[1], K. H. Miller[2], H. Makino[3], D. Craciun[4], D. Simeone[5], V. Craciun[4,*]

[1]Ramapo College of New Jersey, NJ, USA

[2]NASA Goddard Space Flight Center, Greenbelt, MD 20771, USA

[3]Research Institute, Kochi University of Technology, Kami, Kochi, 782-8502, Japan

[4]National Institute for Laser, Plasma, and Radiation Physics, Bucharest-Magurele, Romania

[5]CEA/DEN/DANS/DM2S/SERMA/LEPP-LRC CARMEN CEN Saclay France & CNRS/ SPMS UMR8785 LRC CARMEN, Ecole Centrale de Paris, F92292, Chatenay Malabry.

Abstract

Thin nanocrystalline ZrC and ZrN films (<400 nm), grown on (100) Si substrates at a substrate temperature of 500 ^{o}C by the pulsed laser deposition (PLD) technique, were irradiated by 800 keV Ar ion irradiation with fluences from 1×10^{14} at/cm^2 up to 2×10^{15} at/cm^2. Optical reflectance data, acquired from as-deposited and irradiated films, in the range of 500 - 50000 cm^{-1} (0.06 – 6 eV), was used to assess the effect of irradiation on the optical and electronic properties. Both in ZrC and ZrN films we observed that irradiation affects the optical properties of the films mostly at low frequencies, which is dominated by the free carriers response. In both materials, we found a significant reduction in the free carriers scattering rate, i.e. possible increase in mobility, at higher irradiation flux. This is consistent with our previous findings that irradiation affects the crystallite size and the micro-strain, but it does not induce major structural changes.

Key words: ZrC; ZrN; pulsed laser deposition; nanocristalline films; infrared optical properties

[*]corresponding author; email address: valentin.craciun@inflpr.ro

1. Introduction

Zirconium nitride (ZrN) and zirconium carbide (ZrC) are interesting materials that possess very good ceramic and metallic characteristics such as high melting points [1], high hardness (30-35 GPa) [2, 3], good wear resistance [4], and high thermochemical stability with a single fcc type phase from room temperature up to the melting temperature [5, 6]. Such properties, together with the low neutron cross-section of Zr recommend these films as protective coatings for various applications in nuclear reactors [5-7].

Various deposition techniques have been employed to obtain ZrC and ZrN thin films to investigate their structure, stoichiometry and properties [3-11]. Pulsed laser deposition (PLD) is a very suitable technique for such studies since, by controlling the deposition conditions, films with various structural qualities and compositions can be obtained from a single, inexpensive target [3, 9-11]. We showed previously that ZrC and ZrN films grown by PLD at different temperatures were nanocrystalline and exhibited high hardness and Young's modulus values, low friction coefficients and wear rates [3, 9-11]. We recently investigated the effect of 800 keV Ar ions irradiation on the structural and mechanical properties [12, 13]. We also showed that PLD grown films, being very flat and smooth, with surface rms values of the order of 1 nm, could be investigated with nanometer depth resolution by grazing incidence X-ray diffraction (GIXRD), X-ray reflectivity (XRR) and nanoindentation to observe the effect of irradiation on density, surface morphology, structure and mechanical properties. In this article we investigated the effect of Ar ions irradiation on the optical properties of the irradiated ZrC and ZrN films and compare the results to the previous reported ones [14].

2. Experimental Details

A KrF excimer laser (λ=248 nm, pulse duration τ = 25 ns, 6 J/cm^2 fluence, 40 Hz repetition rate) was used to ablate ZrC and ZrN targets in a stainless steel chamber fitted with several vacuum pumps in order to achieve UHV conditions prior to the deposition of films. The films were deposited for 20,000 pulses at a substrate temperature of 500 ^{o}C under different CH_4 or N_2 pressures [12, 13].

The deposited films were irradiated at room temperature by 800 keV Ar ions at a flux of 10^{11} $cm^{-2}s^{-1}$. For all studied samples, the displacement rate was equal to 4.6×10^{-4} dpa/s. Three distinct irradiations were performed at 4.6 dpa, 46 dpa and 92 dpa (with fluences of 10^{14}, 1×10^{15}, and 2×10^{15} cm^{-2}) in order study the impact of radiation damages on the structure and mechanical properties of the deposited thin films.

Room temperature optical reflectance of the irradiated samples was measured from 500 cm^{-1} to 50 000 cm^{-1} using two spectrometers. A Bruker IFS 125 high-resolution Fourier Transform Spectrometer (FTS) in focused beam (f/6.5) geometry was utilized to cover the frequency band 500-10,000 cm^{-1}. Two combinations of source, beamsplitter, and detector were implemented in the FTS. The frequency range 500-5000 cm^{-1} utilized a globar lamp with a Ge-coated KBr beamsplitter and a room-temperature DLATGS detector. The frequency range 2000-10000 cm^{-1} made use of a tungsten filament source in combination with a CaF2 beamsplitter and a room-temperature DLATGS detector. The frequency band 5000-50000 cm^{-1} was investigated with a Perkin Elmer Lambda 950 Spectrophotometer, employing multiple gratings and detectors (PMT, InGaAs and PbS). For each measurement data from the various ranges agreed to within 0.5% in the overlap regions. The data sets were merged by equating the areas underneath the curves in the overlap regions and using a weighted average to combine data sets.

We mention that both ZrC and ZrN films are the same ones used in our previous optical studies on non-irradiated samples [14]. Because of some small differences between the instruments and the set-ups used in our previous work and in the current one, we measured one non-irradiated sample from the same batch as ZrC1 in the table above and another one from the same batch as ZrN1, and used their optical reflectance for comparison. It must be mentioned that differences between the measurements were observed only at high frequencies, in the near-IR and visible ranges. This is however the spectral region where we found almost no effect due to the irradiation, making our analysis relevant. Room temperature optical reflectance was measured from 30 cm^{-1} (4 meV) to 30 000 cm^{-1} (4 eV), using a Bruker-113v FTIR spectrometer and a Carl Zeiss microscope photometer. Optical conductivity and dielectric constants were obtained from Kramers-Kronig transformation of reflectance data.

High energy X-ray photoelectron spectroscopy (HE-XPS) investigations of the elemental composition and chemical bonding of the films were performed using a custom made laboratory XPS system using a focused monochromatic Cr K_α source (ULVAC-PHI, Inc.) and a wide acceptance angle electron analyzer (VG Scienta EW4000). The X-rays (Cr K_α, hν=5408.5 eV) were focused onto the samples surface in a spot size of around 100 μm diameter. The samples were loaded into the XPS measuring chamber and analyzed without any Ar ion sputtering cleaning procedure, which might have interfered with the measurement. This is a major advantage of HE-XPS measurements, which could analyze much thicker films than the usual XPS machines using Al or Mg X-rays. The core level spectra were recorded at pass energy of 200 eV with a slit-width of 0.8 mm. The electron take-off-angle was 85°, although several angle resolved spectra were also acquired.

3. Results and discussion

Table 1. Deposition conditions and structural properties of the deposited films.

Sample	Atmosphere [mbar]	Grain size [Å]		Micro-strain [%]		Irradiation ion fluence [10^{14}/cm²]
		as-dep	irr	as-dep	irr	
ZrC1	$2x10^{-5}$ CH_4	108	196	0.9	1.1	1
ZrC2	$2x10^{-4}$ CH_4	104	159	0.9	0.9	10
ZrC3	vacuum	107	169	0.8	1.1	20
ZrN1	$2x10^{-3}$ CH_4	110	95	1.2	1.1	1
ZrN3	$2x10^{-3}$ N_2	116	149	1.3	1.1	10

The effect of Ar ions irradiation on the deposited films crystalline structure, grain size, micro-stress values, and mechanical properties, obtained from grazing incidence and symetrical X-ray diffraction (GIXRD and XRD), X-ray reflectivity (XRR) and nanoindentation investigations, were already reported [12, 13]. The results showed that Ar ion irradiation induces grain growth, more so for the ZrC films (see Table 1), a change of relative grains orientation and a marked decrease of the hardness and Young modulus. Also, the surface contamination/oxide layer thickness increases from 2-3 nm to 3-4 nm and its rms roughness as well, from 1 to 2 nm.

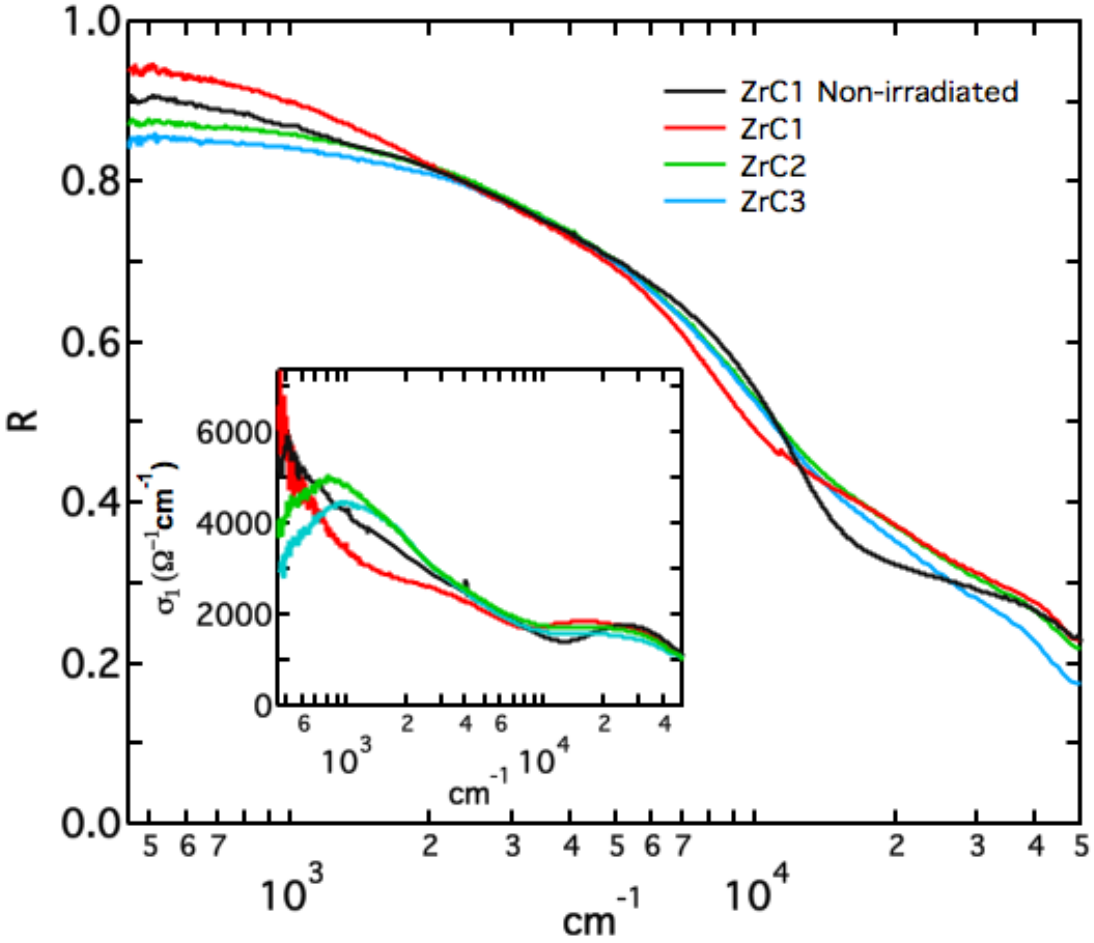

Figure 1. Room temperature optical reflectance R(ω) (main panel) and optical conductivity $\sigma_1(\omega)$ (inset) of the irradiated ZrC thin films, and the non-irradiated ZrC1 sample, as explained in the main text.

Figure 1 shows the measured reflectance (main panel) and the real part of optical conductivity (inset) extracted from Kramers-Kronig transformation for the ZrC samples, including a non-irradiated one from the same batch as ZrC1. In our previous work on non-irradiated films, we found very similar behavior of R(ω) for all three of them (ZrC1, ZrC2 and ZrC3). Therefore, the differences observed in Fig.1 are mainly due to the different irradiation fluencies, as shown in Table 1. At low frequency, optical reflectance apparently increases for low fluency (ZrC1), then it drops with increasing fluency (ZrC2 and ZrC3), but only slightly. It still remains above 85%, suggesting metallic behavior, which is further confirmed by the real part of the dielectric

function $\varepsilon_1(\omega)$ in Fig. 2a. Above the far infrared region (> 600 cm^{-1}), $\varepsilon_1(\omega)$ is negative and increases gradually with frequency. However, Fig. 2a shows that it does not cross the zero value, as expected at the screened plasma frequency of free carriers, but it remains rather negative for the entire measured range. The reason for such behavior is not entirely understood, but we point out that the loss function shown in Fig. 2b, also have unusual behavior. The peak expected at the free carrier plasma frequency is barely distinguishable for the non-irradiated (~12,000 cm^{-1}) and low fluency (~10,000 cm^{-1}) samples, but almost absent for higher fluencies. The reflectance edge around 12,000 cm^{-1}, associated with plasma frequency of free carriers, remains almost un-shifted in position, but it appear to broaden upon irradiation. Above the plasma edge, the same features associated with transitions from the valence band can be identified. The features only shift or broaden slightly, as it is better visible in optical conductivity (inset of Fig. 2).

Also visible in the inset of Fig. 1, there is significant spectral weight shift with irradiation in the far-infrared range, significantly below the onset of the transitions from the valence band. To better understand the effect, we performed a Lorentz-Drude analysis of the data. In the non-irradiated ZrC, similar to our previous work [14], we found a low frequency band centered around 250 cm^{-1}. Although its position is below our lowest measured frequency in this study, the existence of this band is well confirmed by our previous data. After irradiation, the band shifts insignificantly at low irradiation fluency (ZrC1), but its position increases by almost a factor of four (~ 900 cm^{-1}) at higher irradiation fluencies (ZrC2 and ZrC3). Its plasma frequency also increases by more than 10% and it broadens significantly (by more than three times). This is further confirmed by the low frequency behavior of $\varepsilon_1(\omega)$ from Fig. 2a. In the non-irradiated sample, it can be seen the onset of an upturn toward the lowest measured frequency. In ZrC1, i.e. low fluence irradiation, $\varepsilon_1(\omega)$ appears to be dominated by the metallic component, but at higher fluencies, one can see a clear shift of the upturn toward higher frequencies. Most likely, this low frequency band is associated with localized carriers tunneling through the crystallite boundaries. Thus, irradiation produces more charge localization, increasing the tunneling energy, hence the position of the band.

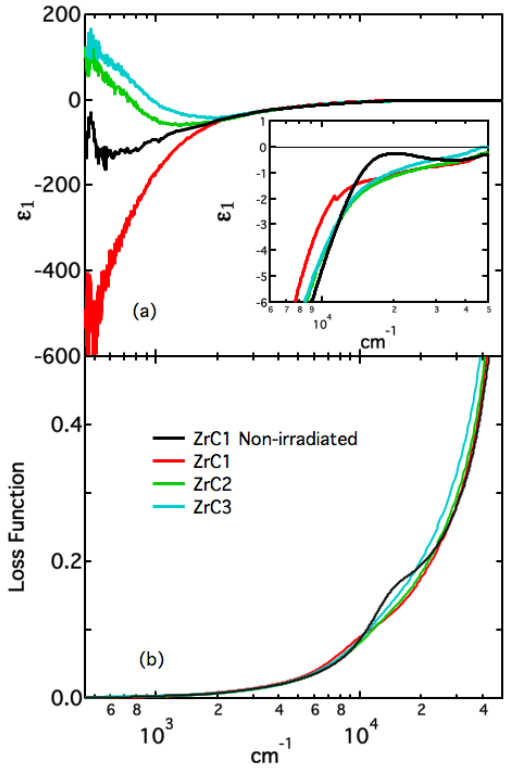

Figure 2. Real part of the dielectric function $\varepsilon_1(\omega)$ (a) and the loss function (b) of the ZrC thin films.

Our results of the fits for the Drude (free carriers) parameters are summarized in Table 2. Drude plasma frequency, hence the free carrier concentration shows a small decrease (within 2%), consistent qualitatively (but not quantitatively) with increased localization. Noticeably, the scattering rate decreases by about a factor of two at high irradiation fluencies, resulting in an enhancement of the zero frequency (dc) conductivity. This may be related to the increase in the crystallite size with irradiation, as reported previously [12], if we consider that conductivity consists of an intra-grain and an inter-grain component. Then, the irradiation would increase the tunneling energy, i.e. reduce the carrier concentration (plasma frequency) through localization. At the same time though, the increase in crystallite size would reduce the number of boundaries, thus reducing the inter-grain scattering, just as we observe in Table 1. A detailed spectral weight analysis would require extension of the measurements at even lower frequencies in the far-infrared region and possibly, even higher irradiation fluencies. Nevertheless, we can conclude that optical spectroscopy is sensitive to and can provide valuable information on the effect of irradiation in ZrC thin films.

	ω_p (eV)	$1/\tau$ (eV)	$\sigma(0)(\Omega^{-1}cm^{-1})$
ZrC1 non-irrad.	1.47 ± 0.05	0.44 ± 0.03	660
ZrC1	1.44 ± 0.05	0.92 ± 0.05	303
ZrC2	1.45 ± 0.05	0.24 ± 0.04	1178
ZrC3	1.45 ± 0.05	0.21 ± 0.04	1346

Table 2. Electrical properties of the irradiated ZrC films extracted from Lorentz-Drude fits of optical conductivity.

Main panel of Fig. 3 shows the reflectance R(ω) of the two irradiated films of ZrN from Table 1, and a non-irradiated one from the same batch as ZrN1. Just as for ZrC, we believe that the differences in optical reflectance between samples are mainly due to the differences between irradiation fluencies. Comparing Fig. 1 and Fig. 3, it can be seen that the low frequency reflectance of ZrN is larger than that of ZrC, exceeding 90% for all samples. Also, the edge associated with plasma frequency of free carriers is much sharper and shifted to higher energy. Both observations are consistent with a higher plasma frequency and a lower scattering rate in ZrN than in ZrC. This is also supported by the optical conductivity data displayed in the inset of Fig. 3, which shows that toward zero frequency, $\sigma_1(\omega)$ has larger values than in the inset of Fig. 1 and it has a sharper drop. As a consequence, unlike in ZrC (Fig. 2a), the dielectric function of ZrN from Fig. 4a has a clear zero crossing at the screened plasma frequency of the conduction carriers, marked with arrows in the inset of Fig. 4a. Furthermore, the loss function of ZrN from Fig. 4b also has a clear peak at the plasma frequency, both for the non-irradiated and the irradiated samples.

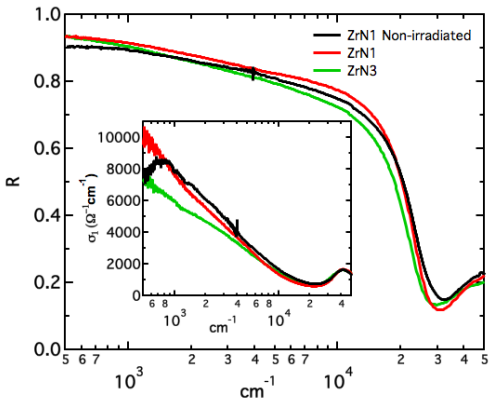

Figure 3. Room temperature optical reflectance R(ω) (main panel) and optical conductivity $\sigma_1(\omega)$ (inset) of the irradiated ZrN thin films, and one non-irradiated, as explained in the main text.

It is worth noticing from the inset of Fig. 3 that the far infrared band, associated with localized charges, appears to be shifted to higher frequency (~900 cm^{-1}) in the non-irradiated ZrN as compared to non-irradiated ZrC. This is also evident from the position of the low frequency upturn of ε_1 from Fig. 4a.

The effect of irradiation on ZrN is clearly visible both in Fig. 3 and Fig. 4. From the main panel of Fig. 3, it can be observed that the reflection edge shifts slightly to lower frequencies and also appears to sharpen. This is consistent with a small reduction of free carriers plasma frequency, but also with a significant loss of scattering, which in turn enhances the low frequency reflectance. Optical conductivity from the inset of Fig. 3 also shows an enhancement toward zero frequency, although non-monotonic with irradiation fluency, just like in ZrC. The small reduction in free carrier plasma frequency is confirmed by the shift of the zero crossing in the inset of Fig. 4a and the shift of the loss function peak in Fig. 4b. The values for the screened plasma frequencies agrees well with previous reports on films obtained by dc magnetron-sputtering [15]. The scattering rates however, are lower by at least a factor of two in our samples, possibly due to larger crystallites in our films. The evolution of plasma frequency is consistent with a reduction of about 10% upon irradiation. Just like in ZrC, irradiation reduces the scattering rate by almost a factor of two. We believe that this is also consistent with the increase in crystallite size by irradiation, as explained above.

Also similar to the effect on ZrC, irradiation shifts the localization band in ZrN toward higher frequencies, possibly explaining the small reduction in plasma frequency. Further confirmation for the spectral weight shift is given by the low frequency behavior of ε_1, which no longer shows the upturn and becomes more negative, being dominated by the metallic character of the sample.

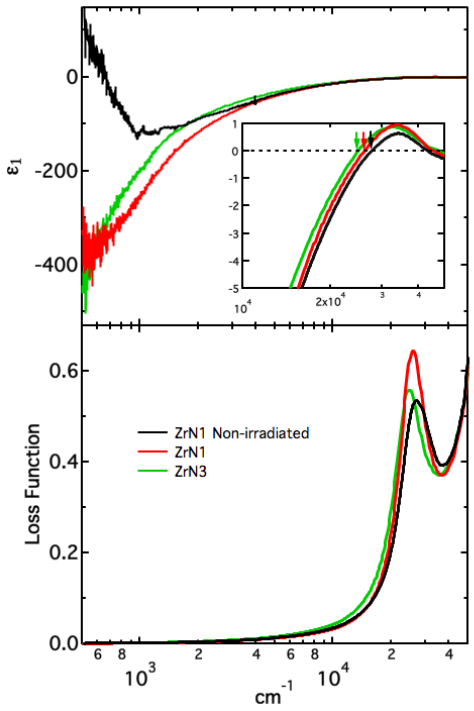

Figure 4. Real part of the dielectric function $\varepsilon_1(\omega)$ (a) and the loss function (b) of the irradiated ZrN thin films.

Almost no changes due to the irradiation can be observed in ZrN at high frequencies in any of the optical properties shown in Figs. 3 and 4. Therefore, we can conclude that irradiation affects mainly the transport properties in both ZrC and ZrN, without major structural, i.e band structure, effects.

	ω_p (eV)	$1/\tau$ (eV)	$\sigma(0)(\Omega^{-1}cm^{-1})$
ZrN1 non-irrad.	3.00 ± 0.05	0.18 ± 0.01	6719
ZrN1	2.65 ± 0.17	0.10 ± 0.01	9439
ZrN3	2.55 ± 0.20	0.10 ± 0.01	8740

Table 3. Electrical properties of the irradiated ZrN films extracted from Lorentz-Drude fits of optical conductivity

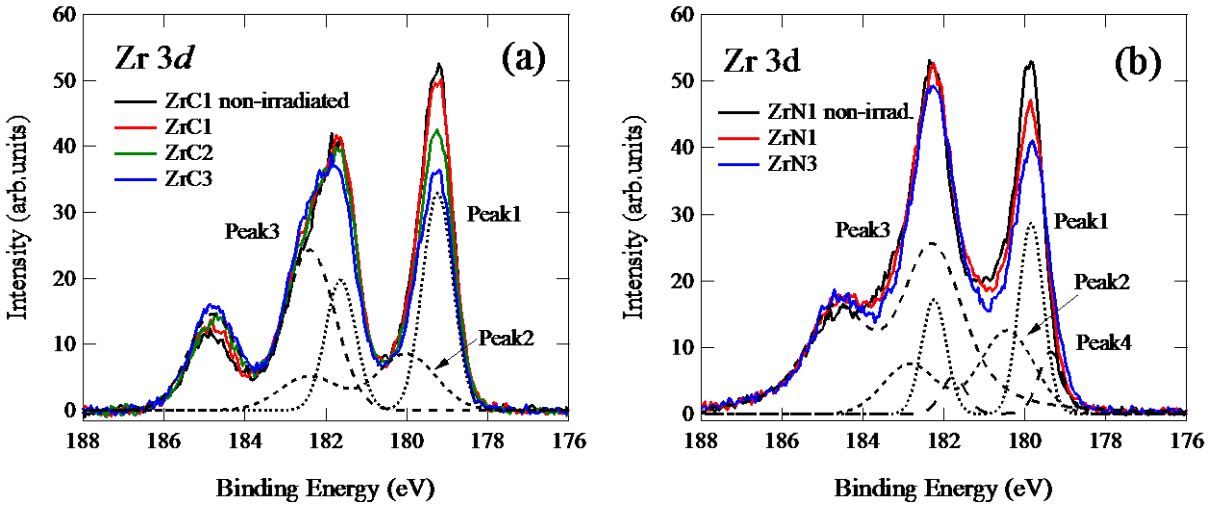

Figure 5. High resolution XPS scans of the Zr 3*d* region for as deposited and irradiated (a) ZrC and (b) ZrN films. Dotted lines show results of peak separation for ZrC3 and ZrN3 films.

High resolution XPS Zr3*d* peaks acquired from the non-irradiated ZrC film and after irradiation are displayed in Fig. 5 (a). The acquired signal could be fit with three pairs of Zr 3*d* peaks, corresponding to Zr-C, Zr-C-O, Zr-O bonds (or Zr-N, Zr-N-O, Zr-O, for the ZrN films as shown in Fig. 5 (b)). According to XPS results, the main effect of the irradiation is the decrease of the Zr-C and Zr-N peaks intensities and the increase of Zr-O-C (Zr-O-N for the ZrN film) and Zr-O peaks intensities. This behavior is very well correlated with the changes of the intensities of the corresponding O 1*s* and C 1*s* peaks, as shown in Fig. 6 (a) and (b) for the ZrC samples. According to our previous results, the ZrC and ZrN films are oxidized only at the surface, oxygen concentration in bulk being quite low, around 1-2 at. % [10, 11]. The oxide and oxycarbide/oxynitride surface layers that form are very dense and block oxygen diffusion. After irradiation, there are many defects near the surface, which will contribute to increased oxygen diffusion into the near surface area, resulting in thicker oxide layers on the samples' surface.

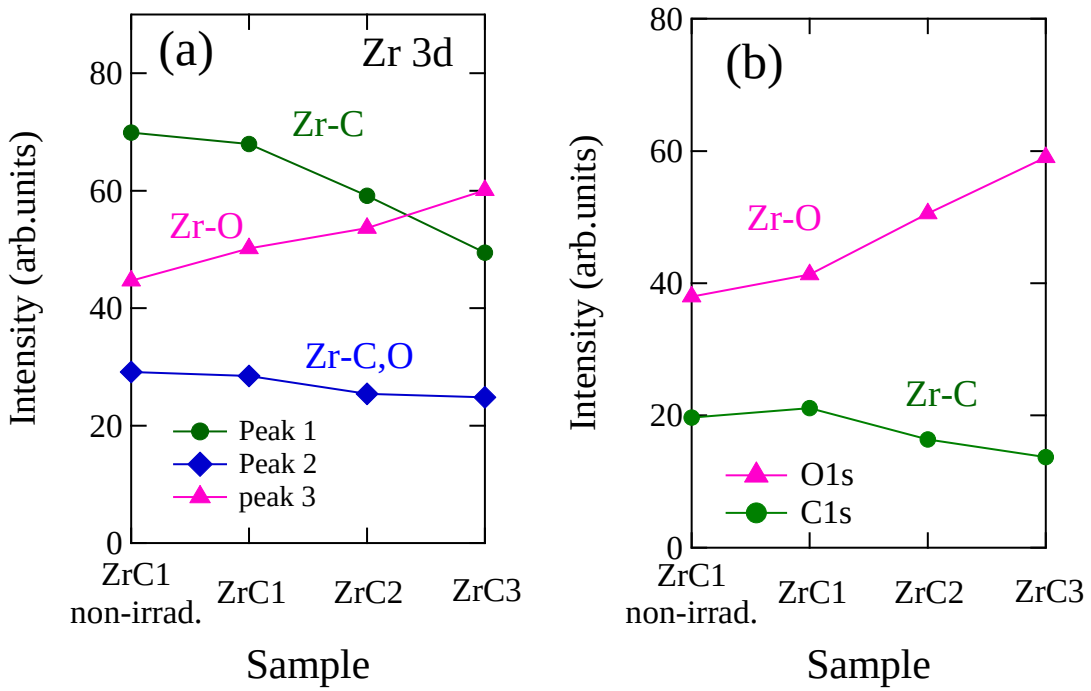

Figure 6. Plot of the areas of (a) Zr 3*d*, (b) O 1*s* and C 1*s* peaks recorded from the non-irradiated and irradiated ZrC films.

At a closer inspection of the Zr 3*d* peaks, those recorded from the ZrN films showed the appearance of a fourth peak, located at 179.34 eV, a lower binding energy than the Zr-N peak located at 179.85 eV as displayed in Fig. 5 (b). This position is very close to the position of Zr-C peak in ZrC located at 179.24 eV; therefore, after irradiation there is a formation of some Zr-C bonds in the ZrN film. The positions and areas of the O 1*s* and C 1*s* also suggest that a Zr-N-C type of compound was formed after the irradiated samples were exposed to the atmosphere. It is clear that ZrN behavior is slightly different than that of ZrC.

4. Conclusions

ZrC films grown on Si substrates using the PLD technique at 500 °C were irradiated by 800 keV Ar ions at fluences from 10^{14} to 2×10^{15} cm^{-2}. Optical reflectometry measurements showed that irradiated films maintained their metallic characteristics, with R values around 0.90 in the infrared range. Almost no changes due to the irradiation can be observed at high frequencies in

any of the optical properties investigated. From the low frequency data a decrease of the electrons scattering rate was inferred, corroborating previous XRD results that showed an increase of the crystalline grains after irradiation. Therefore, we can conclude that irradiation affects mainly the transport properties in both ZrC and ZrN, without major structural, i.e band structure, effects. HE-XPS investigations confirmed that there were no major changes in the chemical bonding of the atoms in the film apart from some increase of the Zr-O along with the irradiation fluence in the surface region. Probably some defects in the surface area allowed for more oxygen diffusion into the films and the growth of the surface oxide layer, confirming previous XRR and AFM measurements.

5. ACKNOWLEDGEMENT: This work was supported by grants of the Romanian Ministry of Education, ROSA STAR project number 60 and NUCLEU program. S.B. would like to thank the financial support from Florida International University Doctoral Evidence Acquisition Fellowship. VC acknowledges the support of the JSPS fellowship S-14058.

6. REFERENCES

[1] L.E. Toth, Transition metal carbides and nitrides, In: Refractory materials: a series of monographs, vol. 7: Academic Press, New York, 1971.

[2] W. Lengauer, Transition metal carbides, nitrides and carbonitrides, In: R. Riedel, editor, Handbook of Ceramic Hard Materials, vol. 1 weinheim: Wiley-VCH 2000.

[3] V. Craciun, E.J. McCumiskey, M. Hanna, C.R. Taylor, Very hard ZrC thin films grown by pulsed laser deposition, Journal of the European Ceramic Society 33 (2013) 2223–2226.

[4] D. Craciun, G. Socol, G. Dorcioman, S. Niculaie, G. Bourne, J. Zhang, E. Lambers, K. Siebein, V. Craciun, Wear resistance of ZrC/TiN and ZrC/ZrN thin multilayers grown by pulsed laser deposition, Applied Physics A 110 (2013) 717–722.

[5] Y. Katoh, G. Vasudevamurthy, T. Nozawa, L.I. Snead, Properties of zirconium carbide for nuclear fuel applications, Journal of Nuclear Materials 441 (2013) 718–742.

[6] Y. Long, A. Javed, J. Chen, Z.K. Chen, X. Xiong, Phase composition, microstructure and mechanical properties of ZrC coatings produced by chemical vapor deposition, Ceramics International 40 (2014) 707–713.

[7] Q.N. Meng, M. Wen, F. Mao, N. Nedfors, U. Jansson, W.T. Zheng, Deposition and characterization of reactive magnetron sputtered zirconium carbide films, Surface and Coatings Technology 232 (2013) 876–883.

[8] C. Liu, B. Liu, Y. Shao, Z.Q. Li, C.H. Tang, Preparation and Characterization of Zirconium Carbide Coating on Coated Fuel Particles, Journal of the American Ceramic Society 90 (2007) 3690–3693.

[9] D. Craciun, G. Socol, N. Stefan, I.N. Mihailescu, G. Bourne, V. Craciun, High-repetition rate pulsed laser deposition of ZrC thin films, Surface and Coatings Technology 203 (2009) 1055–1058.

[10] D. Craciun, G. Bourne, J. Zhang, K. Siebein, G. Socol, G. Dorcioman, V. Craciun, Thin and hard ZrC/TiN multilayers grown by pulsed laser deposition, Surface and Coatings Technology 205 (2011) 5493–5496.

[11] G. Dorcioman, G. Socol, D. Craciun, N. Argibay, E. Lambers, M. Hanna, C.R. Taylor, V. Craciun, Wear tests of ZrC and ZrN thin films grown by pulsed laser deposition, Applied Surface Science 306 (2014) 33–36.

[12] D. Craciun, G. Socol, D. Simeone, S. Behdad, B. Boesl, B.S. Vasile, V. Craciun

Structural and mechanical properties changes induced in nanocrystalline ZrC thin films by Ar ion irradiation, Journal of Nuclear Materials, In Press, Accepted Manuscript, Available online 14 November 2015

[13] D. Craciun, G. Socol, G. Dorcioman, D. Simeone, D. Gosset, S. Behdad, B. Boesl, V. Craciun, Ar ions irradiation effects in ZrN thin films grown by pulsed laser, Applied Surface Science 336 (2015) 129-132.

[14] D. Craciun, G. Socol, E. Lambers, E.J. McCumiskey, C.R. Taylor, C. Martin, N. Argibay, D.B. Tanner, V. Craciun, Optical and mechanical properties of nanocrystalline ZrC thin films grown by pulsed laser deposition, Applied Surface Science 352 (2015) 28-32.

[15] M. Veszelei, K. Andersson, C.-G. Ribbing, K. Jarrendahl, and H. Arwin, Applied Optics 33, No. 10 1993-2001, (1994).